Cell Reports
Report

OPEN ACCESS
CellPress

BIM Is the Primary Mediator of MYC-Induced Apoptosis in Multiple Solid Tissues

Nathiya Muthalagu,[1] Melissa R. Junttila,[2,5] Katrin E. Wiese,[3] Elmar Wolf,[3] Jennifer Morton,[1] Barbara Bauer,[3] Gerard I. Evan,[2,6] Martin Eilers,[3] and Daniel J. Murphy[1,3,4,7,*]

[1]Cancer Research UK Beatson Institute, Garscube Estate, Switchback Road, Glasgow G61 1BD, UK
[2]Helen Diller Family Comprehensive Cancer Center, University of California, San Francisco, 2356 Sutter Street, San Francisco, CA 94115, USA
[3]Theodor Boveri Institute, Biocentre, University of Wuerzburg, Am Hubland, 97074 Wuerzburg, Germany
[4]Institute of Cancer Sciences, University of Glasgow, Garscube Estate, Switchback Road, Glasgow G61 1BD, UK
[5]Present address: Genetech Corp., 1000 New Horizons Way, Vacaville, CA 95688, USA
[6]Present address: Department of Biochemistry, University of Cambridge, 80 Tennis Court Road, Cambridge CB2 1BA, UK
[7]Present address: Institute of Cancer Sciences, CRUK Beatson Institute, University of Glasgow, Garscube Estate, Switchback Road, Glasgow G61 1BD, UK
*Correspondence: daniel.murphy@glasgow.ac.uk
http://dx.doi.org/10.1016/j.celrep.2014.07.057
This is an open access article under the CC BY license (http://creativecommons.org/licenses/by/3.0/).

SUMMARY

MYC is one of the most frequently overexpressed oncogenes in human cancer, and even modestly deregulated MYC can initiate ectopic proliferation in many postmitotic cell types in vivo. Sensitization of cells to apoptosis limits MYC's oncogenic potential. However, the mechanism through which MYC induces apoptosis is controversial. Some studies implicate p19ARF-mediated stabilization of p53, followed by induction of proapoptotic BH3 proteins NOXA and PUMA, whereas others argue for direct regulation of BH3 proteins, especially BIM. Here, we use a single experimental system to systematically evaluate the roles of p19ARF and BIM during MYC-induced apoptosis, in vitro, in vivo, and in combination with a widely used chemotherapeutic, doxorubicin. We find a common specific requirement for BIM during MYC-induced apoptosis in multiple settings, which does not extend to the p53-responsive BH3 family member PUMA, and find no evidence of a role for p19ARF during MYC-induced apoptosis in the tissues examined.

INTRODUCTION

Oncogene-induced tumor suppression presents an efficient cell-autonomous restraint to tumor formation in the face of mitogenic signaling by deregulated proto-oncogenes (Evan et al., 2005). MYC serves as a paradigm example of this phenomenon (Askew et al., 1991; Evan et al., 1992; Strasser et al., 1990): deregulated MYC expression simultaneously drives both cell proliferation and apoptosis, with the relative rates of each ultimately determining whether the affected population expands or contracts. Importantly, the threshold level of MYC required to engage apoptosis is set higher than the level required to initiate cell proliferation, thereby enabling healthy cells to proliferate in response to physiological signaling, all the while maintaining an effective barrier to supraphysiological (i.e., oncogenic) MYC expression (Murphy et al., 2008).

MYC-induced apoptosis is widely thought to be mediated by the ARF-p53 pathway. Overexpression of MYC induces accumulation of p19ARF (p14ARF in human cells), which counteracts MDM2-mediated degradation of p53 (Kamijo et al., 1998; Stott et al., 1998; Zindy et al., 1998; Eischen et al., 1999; Schmitt et al., 1999). Activated p53 in turn induces apoptosis via transcriptional upregulation of BH3-only proteins PUMA and NOXA (Nakano and Vousden, 2001; Villunger et al., 2003). However, apoptosis is not the only possible outcome from p53 stabilization, and recent work has shown that acetylation of K117 (K120 in human p53) is also specifically required for induction of NOXA, PUMA, and thereby apoptosis. Significantly, a K117R mutant p53 is still competent to induce cell-cycle arrest, senescence, and tumor suppression (Li et al., 2012). Thus, a dual-signal mechanism governs cell fate in response to p53 accumulation. Additionally, several groups have reported MYC-induced apoptosis in the absence of either p19ARF or p53, strongly suggesting the existence of an alternative pathway to MYC-induced killing (Hsu et al., 1995; Blyth et al., 2000; Eischen et al., 2001; Finch et al., 2006).

A growing body of evidence supports a central role for the BCL2 homologous (BH) family of proteins in mediating MYC-induced apoptosis. This family of proteins is subdivided into anti-apoptotic (e.g., BCL2, BCLXL, MCL1, and A1), proapoptotic BH3-only (including BIM, BID, BAD, PUMA, and NOXA), and effector BH3 proteins, BAX and BAK. In response to proapoptotic stimuli, BAX and BAK oligomerize to cause mitochondrial outer membrane permeabilization, triggering release of cytochrome *c*, SMAC/DIABLO, and consequent activation of effector caspases (Sarosiek et al., 2013b; Czabotar et al., 2014). Antiapoptotic BH family proteins buffer against pore formation, whereas proapoptotic BH3-only proteins counteract this buffering and, in some instances, can directly stimulate BAX/BAK oligomerization (Llambi et al., 2011; Sarosiek et al., 2013a).

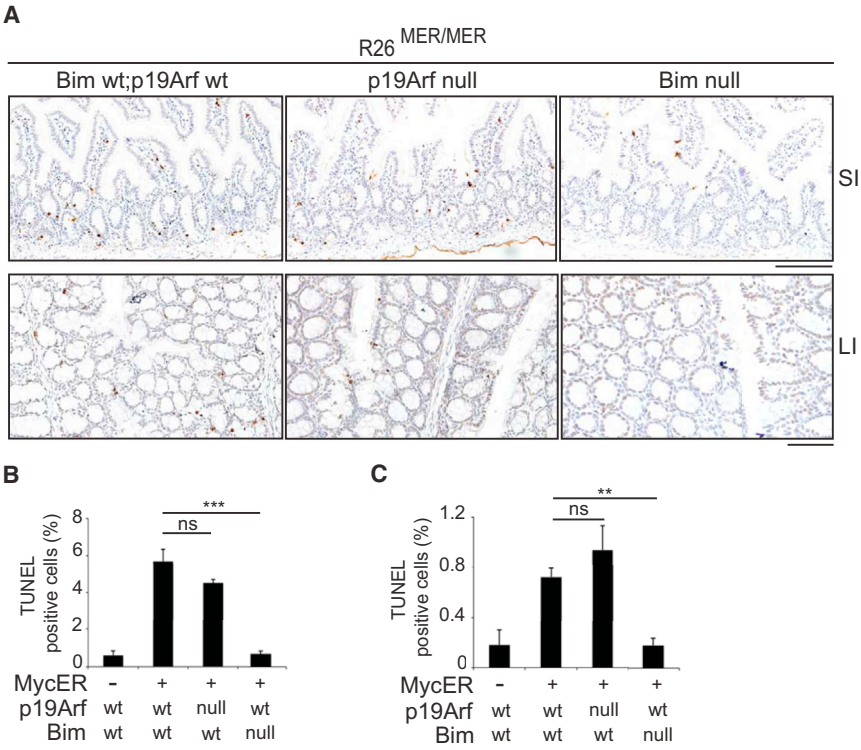

Figure 1. P19ARF Is Dispensable for MYC-Induced Apoptosis in the Intestine

(A) Representative images of TUNEL staining of apoptotic cells in small and large intestine (SI and LI, respectively) of mice of the indicated genotypes, treated daily with Tam (50 mg/kg) to activate MycER^{T2} for 3 days. Scale bars, 100 μm.

(B) Quantification (mean ± SEM) of TUNEL-positive cells (percentage [%] of total) in the small intestine of Tam-treated wild-type (WT) control (n = 3), *R26*$^{MER/MER}$ (n = 3), *R26*$^{MER/MER}$*;Bim* null (n = 4), and *R26*$^{MER/MER}$*;Arf* null (n = 3) mice.

(C) Quantification (mean ± SEM) of TUNEL-positive cells in the large intestine of Tam-treated wild-type control (n = 3), *R26*$^{MER/MER}$ (n = 3), *R26*$^{MER/MER}$*;Bim* null (n = 4), and *R26*$^{MER/MER}$*;Arf* null (n = 3) mice.

Two-tailed, unpaired t tests were used to determine statistical significance: **p < 0.01; ***p < 0.001; ns, not significant.

See also Figure S1.

MYC-induced apoptosis requires BAX/BAK (Dansen et al., 2006; Juin et al., 2002), release of cytochrome *c* (Juin et al., 1999), and activation of effector caspases, contingent upon tonic signaling through CD95 (Hueber et al., 1997), and is blocked by coexpression of antiapoptotic family proteins (Bissonnette et al., 1992; Fanidi et al., 1992; Pelengaris et al., 2002). Conversely, MYC-dependent suppression of BCLXL and BCL2 sensitizes cells to γ-irradiation-induced apoptosis (Eischen et al., 2001; Maclean et al., 2003). The recent identification of *BIM* as a transcriptional target of MYC suggests that this BH3-only protein may directly mediate MYC's proapoptotic signal (Campone et al., 2011; Lee et al., 2013). MYC induces BIM accumulation in Burkitt's lymphoma, and MYC point mutants that fail to induce BIM also fail to induce apoptosis. Notably, such mutants are fully competent to induce p19ARF, p53, and indeed accumulation of p21 downstream of p53 (Hemann et al., 2005). These observations prompted us to reexamine the relative contributions of p19ARF and BIM to MYC-induced apoptosis. We employed here a single transgenic model to systematically evaluate MYC-induced apoptosis in a variety of settings. Our data reveal that BIM is the primary mediator of MYC-induced apoptosis in multiple solid tissues.

RESULTS

BIM Is Required for MYC-Induced Apoptosis in the Intestine

To investigate the mechanistic requirements of MYC-induced apoptosis in multiple tissues, we used a previously described *Rosa26-MycER*^{T2} mouse line that ubiquitously expresses a latent, tamoxifen (Tam)-inducible, chimeric protein comprised of full-length human c-MYC fused to a modified ligand-binding domain from the human estrogen receptor (MycER^{T2}). Deregulated MYC function can thus be induced acutely in *Rosa26-MycER*^{T2} mice by systemic injection of Tam. Owing to the relatively weak activity of the endogenous *Rosa26* promoter, the level of MycER^{T2} expressed is sufficient to drive ectopic proliferation without triggering apoptosis in most adult *R26*$^{MER/MER}$ tissues, with the exception of the small and large intestine, wherein MycER^{T2} is expressed at somewhat higher levels as compared with other tissues. Consequently, activation of MycER^{T2} in the intestine breaches the threshold level of MYC deregulation required to drive apoptosis (Murphy et al., 2008).

To assess the relative contributions of p19ARF and BIM to MYC-induced apoptosis in these tissues, we interbred *Rosa26-MycER*^{T2} mice with *Cdkn2a*$^{tm1(GFP)Cjs}$ (*ARF* ^{GFP}) mice, wherein GFP is inserted into exon 1β of the *Cdkn2a* locus, abrogating p19ARF expression (Zindy et al., 2003), and *Bcl2l11*$^{tm1.1Ast}$ (*BIM*$^{-/-}$) mice (Bouillet et al., 1999), to generate *R26*$^{MER/MER}$*; Arf* $^{GFP/GFP}$ and *R26*$^{MER/MER}$*;Bim*$^{-/-}$ progeny, respectively. MycER^{T2} was induced systemically in adult mice via daily injection with Tam for 3 days, by which time MYC-induced ectopic proliferation peaks, as previously shown (Figure S1A) (Murphy et al., 2008). Tissues were harvested within 24 hr of the final injection, and apoptotic cells were identified by nuclear terminal deoxynucleotidyl transferase dUTP nick end labeling (TUNEL) staining (Figure 1). In the small intestine, MYC-induced apoptosis is largely restricted to the crypt region and was modestly reduced by *Arf* deletion. In the large intestine, where MYC-induced apoptosis is more widely distributed, apoptosis was unaffected by p19ARF loss. Deletion of *Bim* on the other hand abrogated MYC-induced apoptosis in these two tissues.

BIM is thought to act primarily via broad antagonism of prosurvival BH3 family proteins including BCL2, BCLXL, and MCL1,

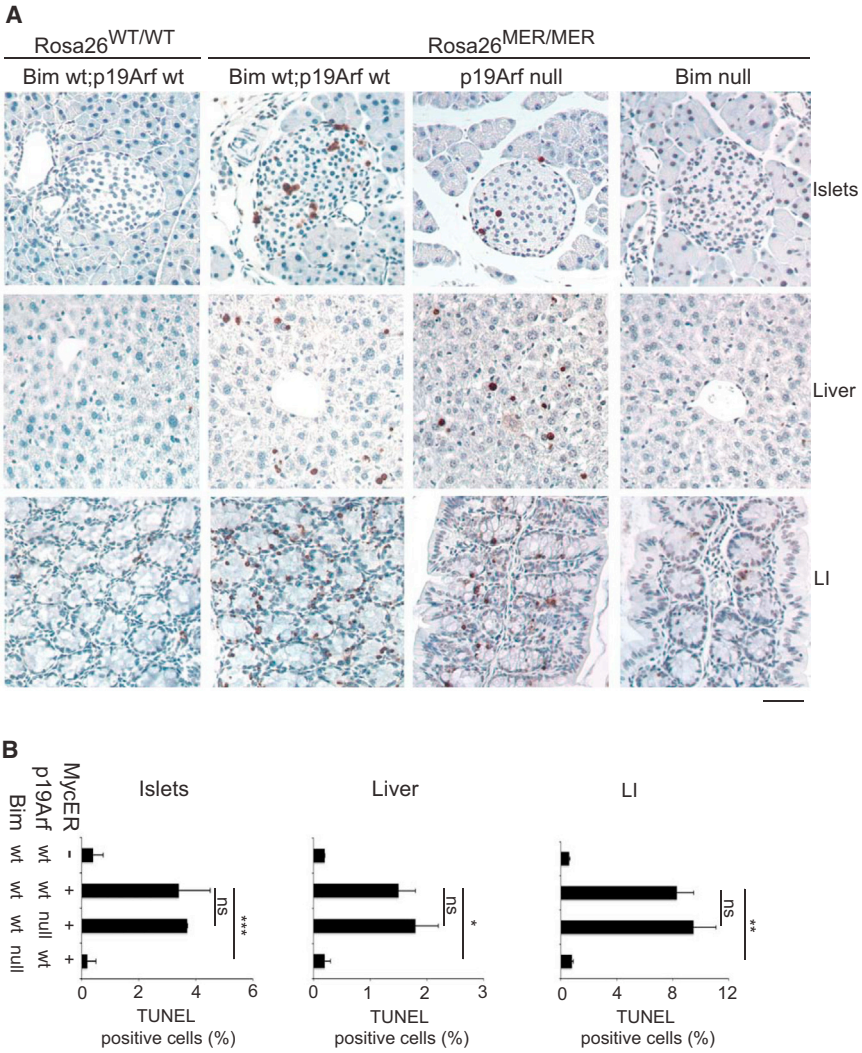

Figure 2. *Bim* Is Required for MYC-Induced Sensitization to Doxorubicin

(A) Representative images of TUNEL staining of apoptotic cells in tissues of mice of the indicated genotypes treated daily with Tam (50 mg/kg) for 3 days and doxorubicin (10 mg/kg) on the third day. Scale bar, 50 μm.

(B) Quantification (mean ± SEM) of TUNEL-positive cells (percentage [%] of total) in the indicated tissues of Tam-and-doxorubicin-treated $R26^{WT/WT}$ control (n = 3), $R26^{MER/MER}$ (n = 3), $R26^{MER/MER}$;*Bim* null (n = 3), and $R26^{MER/MER}$;*Arf* null (n = 5) mice. Two-tailed, unpaired t tests were used to determine statistical significance: *p < 0.05; **p < 0.01; ***p < 0.001; ns, not significant.

See also Figure S2.

although direct activation of the effector BH3 protein BAX likely contributes to BIM's potency (Sarosiek et al., 2013a). PUMA is the primary BH3-only effector of p53-mediated apoptosis in the intestine (Yu et al., 2003). Like BIM, PUMA is a broad specificity antagonist of prosurvival BH3 proteins, and like BIM deletion, PUMA deletion accelerates MYC-induced B cell lymphomagenesis (Michalak et al., 2009). We asked therefore if loss of PUMA (in $Bbc3^{tm1Ast}$ mice) suppresses MYC-induced apoptosis in the intestine. Acute activation of $MycER^{T2}$ in $R26^{MER/MER}$;$Puma^{-/-}$ mice revealed modestly reduced MYC-driven apoptosis in the small intestine, relative to PUMA-replete controls, whereas deletion of *Puma* had no effect on MYC-induced apoptosis in the large intestine (Figures S1B–S1D). Thus, among the proapoptotic BH3-only proteins, there is a specific requirement for BIM during MYC-induced apoptosis in these tissues.

BIM Mediates Proapoptotic Signaling by MYC in Multiple Tissues

The level of $MycER^{T2}$ expressed in other tissues of $R26^{MER/MER}$ mice is alone insufficient to breach the apoptotic threshold but does sensitize cells to additional proapoptotic stimuli, such as doxorubicin (Murphy et al., 2008). To determine if subthreshold apoptotic signaling by MYC is mediated by p19ARF or BIM, we primed $R26^{MER/MER}$;$Arf^{GFP/GFP}$ and $R26^{MER/MER}$;$Bim^{-/-}$ mice by activating $MycER^{T2}$ for 3 days, then treated mice with a dose of doxorubicin that alone fails to drive apoptosis in most tissues. The combination of deregulated MYC and doxorubicin drove measurable apoptosis in liver and pancreatic islets of Langerhans, and enhanced MYC-induced killing in colonic epithelium (Figure 2). Again, deletion of *Bim* abrogated the apoptotic response in all three tissues, whereas disruption of *Arf* had no effect. Deletion of *Puma* protected all three tissues to the same extent as *Bim* loss, confirming the cooperative nature of death in response to these two proapoptotic stimuli (Figure S2A). Notably, however, death induced by doxorubicin alone, confined in these experiments to the small intestine, is unaffected by *Bim* deletion but does require PUMA, as expected for a canonical p53-mediated response to DNA damage (Figure S2B). Moreover, doxorubicin neither induces BIM nor augments MYC induction of BIM protein, and *Bim* is not required for doxorubicin-induced killing in mouse embryonic fibroblasts (MEFs) (Figures S2C and S2D). Thus, MYC and doxorubicin elicit apoptotic signaling via induction of distinct proapoptotic BH3 family proteins.

MYC Directly Regulates BIM Expression

Elevated expression of *Bim-EL* is evident in RNA and protein derived from the small intestine of Tam-treated $R26^{MER/MER}$ mice (Figures S3A and S3B). We generated MEFs from *Rosa26-MycER*^{T2} mice and acutely activated $MycER^{T2}$ with 4-hydroxy-tamoxifen (4-OHT) in vitro to determine if MYC directly regulates *Bim* expression. Increased expression of *Bim-EL* mRNA was found after 6 hr of $MycER^{T2}$ activation and

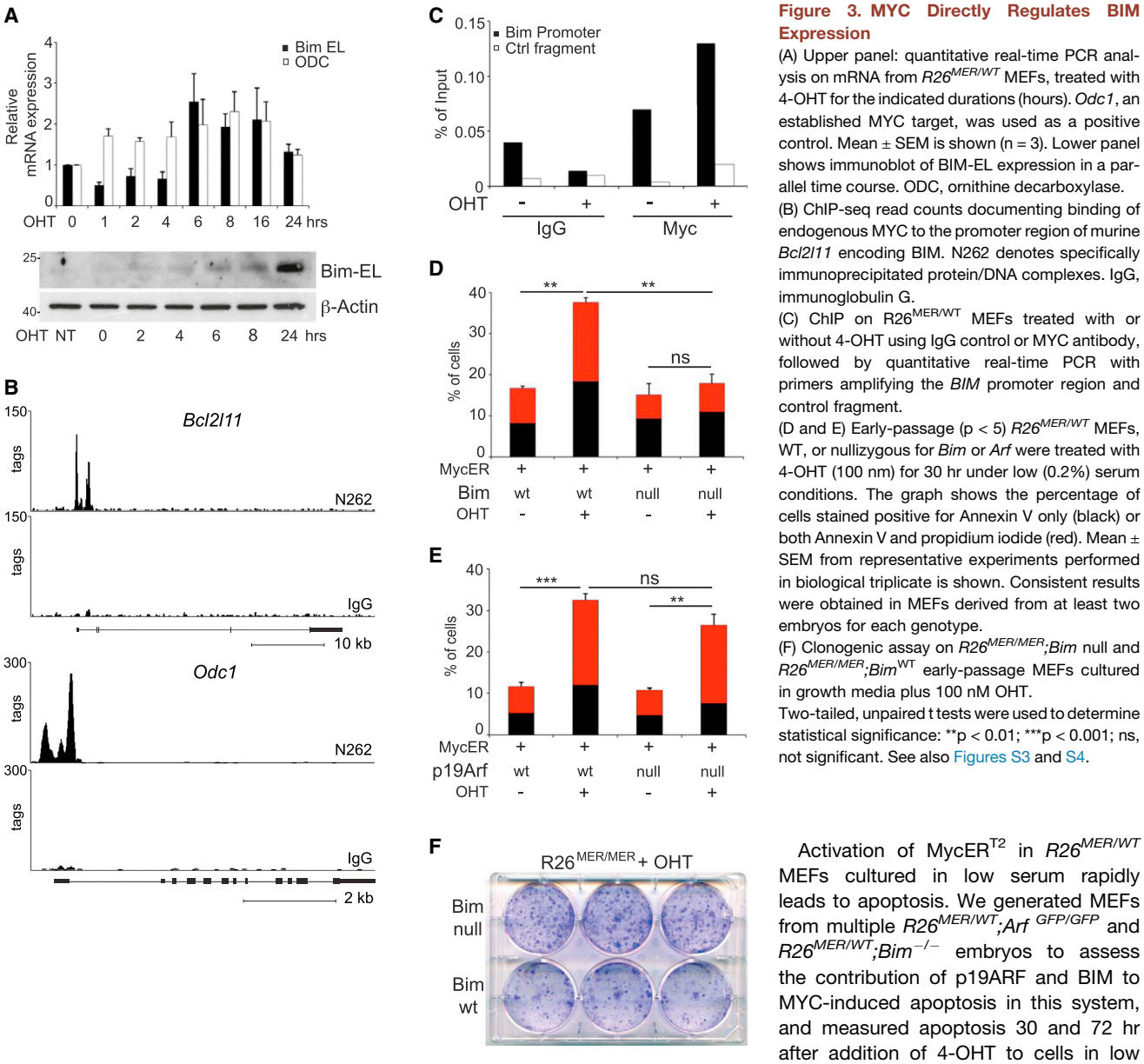

Figure 3. MYC Directly Regulates BIM Expression

(A) Upper panel: quantitative real-time PCR analysis on mRNA from *R26*$^{MER/WT}$ MEFs, treated with 4-OHT for the indicated durations (hours). *Odc1*, an established MYC target, was used as a positive control. Mean ± SEM is shown (n = 3). Lower panel shows immunoblot of BIM-EL expression in a parallel time course. ODC, ornithine decarboxylase.

(B) ChIP-seq read counts documenting binding of endogenous MYC to the promoter region of murine *Bcl2l11* encoding BIM. N262 denotes specifically immunoprecipitated protein/DNA complexes. IgG, immunoglobulin G.

(C) ChIP on R26$^{MER/WT}$ MEFs treated with or without 4-OHT using IgG control or MYC antibody, followed by quantitative real-time PCR with primers amplifying the *BIM* promoter region and control fragment.

(D and E) Early-passage ($p < 5$) *R26*$^{MER/WT}$ MEFs, WT, or nullizygous for *Bim* or *Arf* were treated with 4-OHT (100 nm) for 30 hr under low (0.2%) serum conditions. The graph shows the percentage of cells stained positive for Annexin V only (black) or both Annexin V and propidium iodide (red). Mean ± SEM from representative experiments performed in biological triplicate is shown. Consistent results were obtained in MEFs derived from at least two embryos for each genotype.

(F) Clonogenic assay on *R26*$^{MER/MER}$;*Bim* null and *R26*$^{MER/MER}$;*Bim*^{WT} early-passage MEFs cultured in growth media plus 100 nM OHT.

Two-tailed, unpaired t tests were used to determine statistical significance: $^{**}p < 0.01$; $^{***}p < 0.001$; ns, not significant. See also Figures S3 and S4.

was followed by clear accumulation of BIM-EL protein (Figure 3A). Whole-genome chromatin immunoprecipitation-coupled deep sequencing (ChIP-seq) analysis revealed 4-OHT-induced binding of MycER to the *BIM* (*BCL2L11*) promoter in human MCF10A cells, and constitutive occupation of the *Bim* promoter by endogenous MYC in murine KPC pancreatic tumor cells (Morton et al., 2010), comparable to binding at the canonical MYC target gene *ODC1* (Figures 3B and S3C). Gene-specific ChIP with the N262 antibody, which recognizes both endogenous murine MYC and exogenous MycER^{T2}, revealed increased occupancy of the *Bim* promoter in *R26*$^{MER/WT}$ MEFs in response to 4-OHT (Figure 3C), whereas ChIP analysis in HeLa cells confirmed binding of MYC to the human *BIM* promoter region (Figure S3D), consistent with previous reports by Campone et al. (2011) and Lee et al. (2013).

Activation of MycER^{T2} in *R26*$^{MER/WT}$ MEFs cultured in low serum rapidly leads to apoptosis. We generated MEFs from multiple *R26*$^{MER/WT}$;*Arf* $^{GFP/GFP}$ and *R26*$^{MER/WT}$;*Bim*$^{-/-}$ embryos to assess the contribution of p19ARF and BIM to MYC-induced apoptosis in this system, and measured apoptosis 30 and 72 hr after addition of 4-OHT to cells in low serum. Again, deletion of *Bim* suppressed MYC-induced apoptosis, whereas deletion of *Arf* did not (Figures 3D, 3E, S3E, and S3F). Although serum deprivation alone did induce low levels of BIM expression, further induction of BIM by MYC was unaffected by serum levels (Figure S3G), and, notably, *Bim* deletion had no effect on the basal level of apoptosis induced by culturing MEFs in low serum. Moreover, deletion of *Bim* suppressed MYC sensitization of MEFs cultured in growth media to both γ-irradiation- and ABT-737-induced apoptosis (Figure S4), and *Bim* null MEFs showed increased clonogenic survival in the presence of deregulated MYC (Figure 3F).

A Threshold Level of BIM Is Required for MYC-Induced Apoptosis

Activation of MycER^{T2} in heterozygous *R26*$^{MER/WT}$ mice fails to induce enterocyte apoptosis, whereas apoptosis is readily

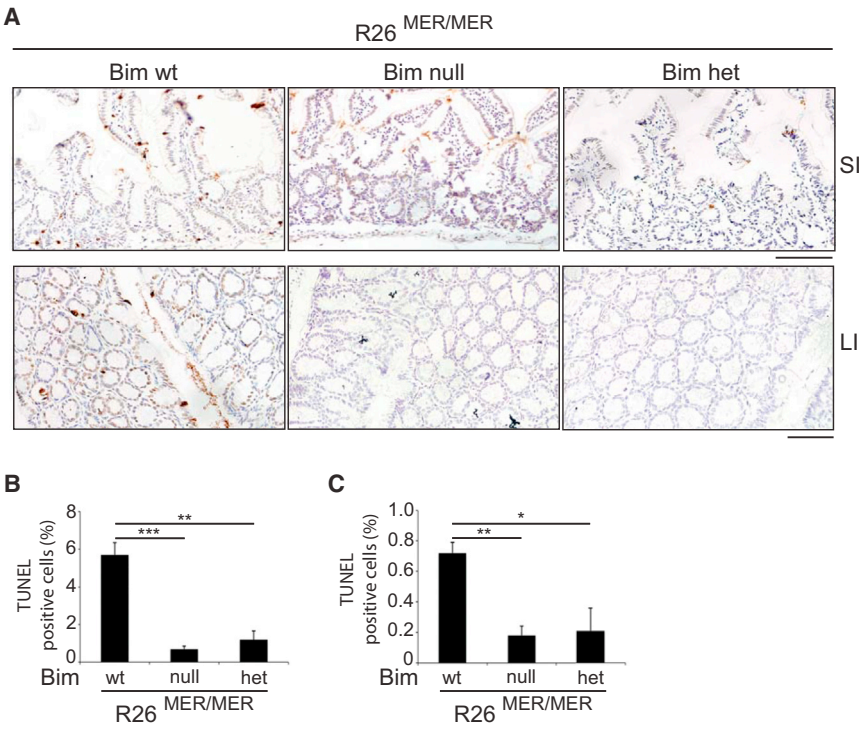

Figure 4. BIM Is Dose Limiting for MYC-Induced Apoptosis

(A) Representative images of TUNEL staining of apoptotic cells in small and large intestine (SI and LI, respectively) of mice of the indicated genotypes, treated daily with Tam (50 mg/kg) to activate MycER^{T2} for 3 days. Scale bars, 100 μm.

(B) Quantification (mean ± SEM) of TUNEL-positive cells in the small intestine of Tam-treated *R26*$^{MER/MER}$ (n = 3), *R26*$^{MER/MER}$;*Bim* null (n = 4), and *R26*$^{MER/MER}$;*Bim* heterozygous (n = 3) mice.

(C) Quantification (mean ± SEM) of TUNEL-positive cells in the large intestine of Tam-treated *R26*$^{MER/MER}$ (n = 3) *R26*$^{MER/MER}$;*Bim* null (n = 4), and *R26*$^{MER/MER}$;*Bim* heterozygous (n = 3) mice.

Two-tailed, unpaired t tests were used to determine statistical significance: *p < 0.05; **p < 0.01; ***p < 0.001.

detected in the same tissue of Tam-treated homozygous *R26*$^{MER/MER}$ mice, indicating that a threshold level of MYC deregulation is required for this effect (Murphy et al., 2008). We therefore asked if reducing *Bim* expression would attenuate the proapoptotic signal emanating from MYC deregulation to a level below this threshold and thereby protect *R26*$^{MER/MER}$ intestines from apoptosis. Comparing levels of apoptosis across *R26*$^{MER/MER}$;*Bim*$^{-/-}$, *R26*$^{MER/MER}$;*Bim*$^{+/-}$, and *R26*$^{MER/MER}$;*Bim*^{WT} mice, it is clear that haploinsufficiency for *Bim* rescues *R26*$^{MER/MER}$ intestines from MYC-induced apoptosis (Figure 4). This result is in broad agreement with a previous report that haploinsufficiency for *Bim* accelerates MYC-induced lymphomagenesis and supports a model where a threshold level of BIM is required to mediate MYC's apoptotic signal (Egle et al., 2004).

DISCUSSION

We present here evidence that the BH3-only protein BIM is the primary mediator of MYC-induced apoptosis in vivo and in vitro. We show MYC binding to the *BIM* promoter, acutely elevating BIM expression, and provide genetic evidence that BIM is required for MYC-induced apoptosis under multiple circumstances and in multiple solid tissues. Strikingly, deletion of *Puma* fails to phenocopy *Bim* deletion when apoptosis is induced by MYC alone, despite the fact that loss of PUMA, like loss of BIM, has been shown to accelerate MYC-induced lymphomagenesis and despite similarities in their mechanism of action (Egle et al., 2004; Czabotar et al., 2014). Conversely, *Bim* deletion fails to phenocopy PUMA loss during doxorubicin-induced apoptosis in the small intestine. However, both BIM and PUMA are required for the synthetic induction of apoptosis driven by the combination of MYC and doxorubicin in tissues where either alone is insufficient to trigger cell death. The differential sensitivities of various tissues to experimental apoptotic stimuli are partly explained by differences in MycER^{T2} expression levels (Murphy et al., 2008) but also likely reflect the level of apoptotic priming intrinsic to each tissue, where differential expression of specific antiapoptotic BH3 proteins may determine the relative potency of individual proapoptotic BH3 proteins (Ni Chonghaile et al., 2011). Thus, these results argue for a model wherein individual BH3-only proteins have evolved to transduce specific proapoptotic signals yet can combine to overcome antiapoptotic buffering.

Therapeutic Implications

MYC family oncogenes are among the most frequently overexpressed genes across a broad spectrum of human cancers. Effective MYC-centric therapies could therefore have a tremendous impact on cancer survival rates. Several strategies to target MYC are being actively pursued, including direct suppression of MYC protein (Soucek et al., 2008; Popov et al., 2010), transcriptional suppression (Zuber et al., 2011), and synthetic lethality (Goga et al., 2007; Liu et al., 2012; Kemp and Grandori, 2013), and it is likely that combinatorial strategies will ultimately prove the most effective. A rational strategy to exploit the intrinsic apoptotic potential of MYC-overexpressing cells would complement these efforts greatly. BH3 mimetics suppress lymphomagenesis in Eμ-MYC mice, even in the absence of a functional p53 pathway (Kelly et al., 2013, 2014). Given the prevalence of MYC overexpression in human cancers, our data support the approach of augmenting the intrinsic apoptotic response through the use of BH3 mimetics and suggest that this strategy may elicit therapeutic benefits in a spectrum of solid tumor types.

EXPERIMENTAL PROCEDURES

Genetically Engineered Mice and Mouse Procedures

Rosa26-MycER^{T2} (Murphy et al., 2008), *Cdkn2a*$^{tm1(GFP)Cjs}$ (*Arf* ^{GFP}; NCI Mouse Repository; Zindy et al., 2003), *Bcl2l11*$^{tm1.1Ast}$ (*Bim*^{Null}; Jackson Laboratory; Bouillet et al., 1999), and *Bbc3*^{tm1Ast} (*Puma*^{Null}; Jackson Laboratory, distributed by Charles River; Villunger et al., 2003) mice were maintained on a C57/bl6 background, housed on a 12 hr light cycle, and fed and watered ad libitum. Procedures involving mice were performed in accordance with protocol numbers AN 076148 (UCSF IACUC, USA) and 55.2-2531.01-30/11 (University of Wuerzburg, Germany) and Home Office license number 60/4183 (CRUK BICR, UK) and approved by the local animal research committees at all three locations. All treatments were performed on mice aged 8–12 weeks. Tam (Sigma-Aldrich) dissolved in peanut oil was administered once a day by intraperitoneal injection for 3 days at 50 mg/kg. Doxorubicin (LC Laboratories) dissolved in 0.9% NaCl was administered once by intraperitoneal injection at 10 mg/kg. Tissues were fixed overnight in zinc-buffered formalin (Thermo Scientific; 5701ZF).

Immunohistochemistry

TUNEL staining was performed on paraffin-embedded sections (4 μm thick) using the ApopTag peroxidase labeling kit (Millipore; S7100). An additional blocking step (1% BSA for 1 hr at room temperature) was incorporated prior to addition of peroxidase-conjugated antidigoxigenin. Tissues were counterstained in Gil 1 hematoxylin followed by blueing solution. For quantification, the number of TUNEL-positive nuclei (pyknotic or intact) and the total number of cells per 20× field were counted manually. Five representative fields per tissue sample from each mouse were scored, yielding a percent apoptosis value. Graphs represent the mean ± SEM percent apoptosis across number ("n") of mice as indicated in the figure legends.

ACCESSION NUMBERS

Complete ChIP-seq data sets can be accessed in the Gene Expression Omnibus database under accession numbers GSE44672 (mouse) and GSE59001 (human).

SUPPLEMENTAL INFORMATION

Supplemental Information includes Supplemental Experimental Procedures and four figures and can be found with this article online at http://dx.doi.org/10.1016/j.celrep.2014.07.057.

AUTHOR CONTRIBUTIONS

D.J.M., M.J., G.I.E., and M.E. conceived the project. N.M., M.J., K.E.W., J.M., E.W., B.B., and D.J.M. performed the experiments. All authors contributed to the interpretation of results. N.M. and D.J.M. wrote the manuscript.

ACKNOWLEDGMENTS

We wish to thank Stephen Tait and Catherine Winchester for careful reading of this manuscript and Gabriel Kalna for advice on the use of statistics. Special thanks to Fanya Rostker, Angela Gruen, Christine Kraemer, Derek Miller, and all the staff of the Beatson Institute Animal Services Unit for animal husbandry; Colin Nixon and the BICR Histology Core; the Beatson Advanced Imaging Resource for advice on microscopy; and Jannes Ulbrich and Alasdair Fraser for technical assistance. Funding for this project was provided by the NIH (R01-CA106526 to G.I.E.) and Deutsche Krebshilfe (109220 to D.J.M.). N.M. was supported by the University of Wuerzburg GSLS and a CRUK Beatson Studentship. M.J. was supported by the Enrique Cepero Fellowship from the Damon Runion Cancer Research Foundation. K.E.W., E.W., and M.E. were supported by DFG grant Ei222/12-1.

Received: March 7, 2014
Revised: June 4, 2014
Accepted: July 30, 2014
Published: August 28, 2014

REFERENCES

Askew, D.S., Ashmun, R.A., Simmons, B.C., and Cleveland, J.L. (1991). Constitutive c-myc expression in an IL-3-dependent myeloid cell line suppresses cell cycle arrest and accelerates apoptosis. Oncogene *6*, 1915–1922.

Bissonnette, R.P., Echeverri, F., Mahboubi, A., and Green, D.R. (1992). Apoptotic cell death induced by c-myc is inhibited by bcl-2. Nature *359*, 552–554.

Blyth, K., Stewart, M., Bell, M., James, C., Evan, G., Neil, J.C., and Cameron, E.R. (2000). Sensitivity to myc-induced apoptosis is retained in spontaneous and transplanted lymphomas of CD2-mycER mice. Oncogene *19*, 773–782.

Bouillet, P., Metcalf, D., Huang, D.C., Tarlinton, D.M., Kay, T.W., Köntgen, F., Adams, J.M., and Strasser, A. (1999). Proapoptotic Bcl-2 relative Bim required for certain apoptotic responses, leukocyte homeostasis, and to preclude autoimmunity. Science *286*, 1735–1738.

Campone, M., Noël, B., Couriaud, C., Grau, M., Guillemin, Y., Gautier, F., Gouraud, W., Charbonnel, C., Campion, L., Jézéquel, P., et al. (2011). c-Myc dependent expression of pro-apoptotic Bim renders HER2-overexpressing breast cancer cells dependent on anti-apoptotic Mcl-1. Mol. Cancer *10*, 110.

Czabotar, P.E., Lessene, G., Strasser, A., and Adams, J.M. (2014). Control of apoptosis by the BCL-2 protein family: implications for physiology and therapy. Nat. Rev. Mol. Cell Biol. *15*, 49–63.

Dansen, T.B., Whitfield, J., Rostker, F., Brown-Swigart, L., and Evan, G.I. (2006). Specific requirement for Bax, not Bak, in Myc-induced apoptosis and tumor suppression in vivo. J. Biol. Chem. *281*, 10890–10895.

Egle, A., Harris, A.W., Bouillet, P., and Cory, S. (2004). Bim is a suppressor of Myc-induced mouse B cell leukemia. Proc. Natl. Acad. Sci. USA *101*, 6164–6169.

Eischen, C.M., Weber, J.D., Roussel, M.F., Sherr, C.J., and Cleveland, J.L. (1999). Disruption of the ARF-Mdm2-p53 tumor suppressor pathway in Myc-induced lymphomagenesis. Genes Dev. *13*, 2658–2669.

Eischen, C.M., Woo, D., Roussel, M.F., and Cleveland, J.L. (2001). Apoptosis triggered by Myc-induced suppression of Bcl-X(L) or Bcl-2 is bypassed during lymphomagenesis. Mol. Cell. Biol. *21*, 5063–5070.

Evan, G.I., Wyllie, A.H., Gilbert, C.S., Littlewood, T.D., Land, H., Brooks, M., Waters, C.M., Penn, L.Z., and Hancock, D.C. (1992). Induction of apoptosis in fibroblasts by c-myc protein. Cell *69*, 119–128.

Evan, G.I., Christophorou, M., Lawlor, E.A., Ringshausen, I., Prescott, J., Dansen, T., Finch, A., Martins, C., and Murphy, D. (2005). Oncogene-dependent tumor suppression: using the dark side of the force for cancer therapy. Cold Spring Harb. Symp. Quant. Biol. *70*, 263–273.

Fanidi, A., Harrington, E.A., and Evan, G.I. (1992). Cooperative interaction between c-myc and bcl-2 proto-oncogenes. Nature *359*, 554–556.

Finch, A., Prescott, J., Shchors, K., Hunt, A., Soucek, L., Dansen, T.B., Swigart, L.B., and Evan, G.I. (2006). Bcl-xL gain of function and p19 ARF loss of function cooperate oncogenically with Myc in vivo by distinct mechanisms. Cancer Cell *10*, 113–120.

Goga, A., Yang, D., Tward, A.D., Morgan, D.O., and Bishop, J.M. (2007). Inhibition of CDK1 as a potential therapy for tumors over-expressing MYC. Nat. Med. *13*, 820–827.

Hemann, M.T., Bric, A., Teruya-Feldstein, J., Herbst, A., Nilsson, J.A., Cordon-Cardo, C., Cleveland, J.L., Tansey, W.P., and Lowe, S.W. (2005). Evasion of the p53 tumour surveillance network by tumour-derived MYC mutants. Nature *436*, 807–811.

Hsu, B., Marin, M.C., el-Naggar, A.K., Stephens, L.C., Brisbay, S., and McDonnell, T.J. (1995). Evidence that c-myc mediated apoptosis does not require wild-type p53 during lymphomagenesis. Oncogene *11*, 175–179.

Hueber, A.O., Zörnig, M., Lyon, D., Suda, T., Nagata, S., and Evan, G.I. (1997). Requirement for the CD95 receptor-ligand pathway in c-Myc-induced apoptosis. Science *278*, 1305–1309.

Juin, P., Hueber, A.O., Littlewood, T., and Evan, G. (1999). c-Myc-induced sensitization to apoptosis is mediated through cytochrome c release. Genes Dev. *13*, 1367–1381.

Juin, P., Hunt, A., Littlewood, T., Griffiths, B., Swigart, L.B., Korsmeyer, S., and Evan, G. (2002). c-Myc functionally cooperates with Bax to induce apoptosis. Mol. Cell. Biol. *22*, 6158–6169.

Kamijo, T., Weber, J.D., Zambetti, G., Zindy, F., Roussel, M.F., and Sherr, C.J. (1998). Functional and physical interactions of the ARF tumor suppressor with p53 and Mdm2. Proc. Natl. Acad. Sci. USA *95*, 8292–8297.

Kelly, P.N., Grabow, S., Delbridge, A.R., Adams, J.M., and Strasser, A. (2013). Prophylactic treatment with the BH3 mimetic ABT-737 impedes Myc-driven lymphomagenesis in mice. Cell Death Differ. *20*, 57–63.

Kelly, G.L., Grabow, S., Glaser, S.P., Fitzsimmons, L., Aubrey, B.J., Okamoto, T., Valente, L.J., Robati, M., Tai, L., Fairlie, W.D., et al. (2014). Targeting of MCL-1 kills MYC-driven mouse and human lymphomas even when they bear mutations in p53. Genes Dev. *28*, 58–70.

Kemp, C.J., and Grandori, C. (2013). Functional genomics to identify unforeseen cancer drug targets. Future Oncol. *9*, 473–476.

Lee, Y.Y., Moujalled, D., Doerflinger, M., Gangoda, L., Weston, R., Rahimi, A., de Alboran, I., Herold, M., Bouillet, P., Xu, Q., et al. (2013). CREB-binding protein (CBP) regulates β-adrenoceptor (β-AR)-mediated apoptosis. Cell Death Differ. *20*, 941–952.

Li, T., Kon, N., Jiang, L., Tan, M., Ludwig, T., Zhao, Y., Baer, R., and Gu, W. (2012). Tumor suppression in the absence of p53-mediated cell-cycle arrest, apoptosis, and senescence. Cell *149*, 1269–1283.

Liu, L., Ulbrich, J., Müller, J., Wüstefeld, T., Aeberhard, L., Kress, T.R., Muthalagu, N., Rycak, L., Rudalska, R., Moll, R., et al. (2012). Deregulated MYC expression induces dependence upon AMPK-related kinase 5. Nature *483*, 608–612.

Llambi, F., Moldoveanu, T., Tait, S.W., Bouchier-Hayes, L., Temirov, J., McCormick, L.L., Dillon, C.P., and Green, D.R. (2011). A unified model of mammalian BCL-2 protein family interactions at the mitochondria. Mol. Cell *44*, 517–531.

Maclean, K.H., Keller, U.B., Rodriguez-Galindo, C., Nilsson, J.A., and Cleveland, J.L. (2003). c-Myc augments gamma irradiation-induced apoptosis by suppressing Bcl-XL. Mol. Cell. Biol. *23*, 7256–7270.

Michalak, E.M., Jansen, E.S., Happo, L., Cragg, M.S., Tai, L., Smyth, G.K., Strasser, A., Adams, J.M., and Scott, C.L. (2009). Puma and to a lesser extent Noxa are suppressors of Myc-induced lymphomagenesis. Cell Death Differ. *16*, 684–696.

Morton, J.P., Timpson, P., Karim, S.A., Ridgway, R.A., Athineos, D., Doyle, B., Jamieson, N.B., Oien, K.A., Lowy, A.M., Brunton, V.G., et al. (2010). Mutant p53 drives metastasis and overcomes growth arrest/senescence in pancreatic cancer. Proc. Natl. Acad. Sci. USA *107*, 246–251.

Murphy, D.J., Junttila, M.R., Pouyet, L., Karnezis, A., Shchors, K., Bui, D.A., Brown-Swigart, L., Johnson, L., and Evan, G.I. (2008). Distinct thresholds govern Myc's biological output in vivo. Cancer Cell *14*, 447–457.

Nakano, K., and Vousden, K.H. (2001). PUMA, a novel proapoptotic gene, is induced by p53. Mol. Cell *7*, 683–694.

Ni Chonghaile, T., Sarosiek, K.A., Vo, T.T., Ryan, J.A., Tammareddi, A., Moore, Vdel.G., Deng, J., Anderson, K.C., Richardson, P., Tai, Y.T., et al. (2011). Pretreatment mitochondrial priming correlates with clinical response to cytotoxic chemotherapy. Science *334*, 1129–1133.

Pelengaris, S., Khan, M., and Evan, G.I. (2002). Suppression of Myc-induced apoptosis in beta cells exposes multiple oncogenic properties of Myc and triggers carcinogenic progression. Cell *109*, 321–334.

Popov, N., Schülein, C., Jaenicke, L.A., and Eilers, M. (2010). Ubiquitylation of the amino terminus of Myc by SCF(β-TrCP) antagonizes SCF(Fbw7)-mediated turnover. Nat. Cell Biol. *12*, 973–981.

Sarosiek, K.A., Chi, X., Bachman, J.A., Sims, J.J., Montero, J., Patel, L., Flanagan, A., Andrews, D.W., Sorger, P., and Letai, A. (2013a). BID preferentially activates BAK while BIM preferentially activates BAX, affecting chemotherapy response. Mol. Cell *51*, 751–765.

Sarosiek, K.A., Ni Chonghaile, T., and Letai, A. (2013b). Mitochondria: gatekeepers of response to chemotherapy. Trends Cell Biol. *23*, 612–619.

Schmitt, C.A., McCurrach, M.E., de Stanchina, E., Wallace-Brodeur, R.R., and Lowe, S.W. (1999). INK4a/ARF mutations accelerate lymphomagenesis and promote chemoresistance by disabling p53. Genes Dev. *13*, 2670–2677.

Soucek, L., Whitfield, J., Martins, C.P., Finch, A.J., Murphy, D.J., Sodir, N.M., Karnezis, A.N., Swigart, L.B., Nasi, S., and Evan, G.I. (2008). Modelling Myc inhibition as a cancer therapy. Nature *455*, 679–683.

Stott, F.J., Bates, S., James, M.C., McConnell, B.B., Starborg, M., Brookes, S., Palmero, I., Ryan, K., Hara, E., Vousden, K.H., and Peters, G. (1998). The alternative product from the human CDKN2A locus, p14(ARF), participates in a regulatory feedback loop with p53 and MDM2. EMBO J. *17*, 5001–5014.

Strasser, A., Harris, A.W., Bath, M.L., and Cory, S. (1990). Novel primitive lymphoid tumours induced in transgenic mice by cooperation between myc and bcl-2. Nature *348*, 331–333.

Villunger, A., Michalak, E.M., Coultas, L., Müllauer, F., Böck, G., Ausserlechner, M.J., Adams, J.M., and Strasser, A. (2003). p53- and drug-induced apoptotic responses mediated by BH3-only proteins puma and noxa. Science *302*, 1036–1038.

Yu, J., Wang, Z., Kinzler, K.W., Vogelstein, B., and Zhang, L. (2003). PUMA mediates the apoptotic response to p53 in colorectal cancer cells. Proc. Natl. Acad. Sci. USA *100*, 1931–1936.

Zindy, F., Eischen, C.M., Randle, D.H., Kamijo, T., Cleveland, J.L., Sherr, C.J., and Roussel, M.F. (1998). Myc signaling via the ARF tumor suppressor regulates p53-dependent apoptosis and immortalization. Genes Dev. *12*, 2424–2433.

Zindy, F., Williams, R.T., Baudino, T.A., Rehg, J.E., Skapek, S.X., Cleveland, J.L., Roussel, M.F., and Sherr, C.J. (2003). Arf tumor suppressor promoter monitors latent oncogenic signals in vivo. Proc. Natl. Acad. Sci. USA *100*, 15930–15935.

Zuber, J., Shi, J., Wang, E., Rappaport, A.R., Herrmann, H., Sison, E.A., Magoon, D., Qi, J., Blatt, K., Wunderlich, M., et al. (2011). RNAi screen identifies Brd4 as a therapeutic target in acute myeloid leukaemia. Nature *478*, 524–528.